Bulk quantum Hall effect in η-Mo_4O_{11}

S. Hill
Department of Physics, Montana State University, Bozeman, Montana 59717

S. Uji, M. Takashita, C. Terakura, T. Terashima, and H. Aoki
National Research Institute for Metals, Tsukuba, Ibaraki 305, Japan

J. S. Brooks
Department of Physics and National High Magnetic Field Laboratory, Florida State University, Tallahassee, Florida 32310

Z. Fisk
Department of Physics and National High Magnetic Field Laboratory, Florida State University, Tallahassee, Florida 32310

J. Sarrao
Los Alamos National Labs, MST-10, Mail Stop K764, Los Alamos, New Mexico 87545

(Received 1 June 1998)

We report the observation of a bulk quantum Hall effect in the quasi-two-dimensional conductor η-Mo_4O_{11}. The Hall resistance exhibits well-defined quantized plateaus, coincident with pronounced minima in the diagonal resistance. We propose a model involving (i) tiny quasi-two-dimensional electron and hole pockets, left over from an imperfectly nested charge-density wave, and (ii) the exchange of carriers between these mobile states and the localized charge-density-wave condensate. Together with a magnetic field, these factors result in well-separated bands of mobile states superimposed on a background continuum of localized states—the key ingredients for a quantum Hall effect. We also discuss the implications of these findings in the light of recent predictions concerning chiral metallic surface states in bulk quantum Hall systems. [S0163-1829(98)06140-2]

I. INTRODUCTION

A strictly two-dimensional (2D) conducting system, subjected to a perpendicular magnetic field, exhibits a quantum Hall effect (QHE) when the orbital (and Zeeman) magnetic energy becomes comparable to the electronic (Fermi) energy, i.e., when the so-called quantum limit is reached.[1–3] The magnetic field completely quantizes the locally available electronic states of the system, opening up clear gaps in its excitation spectrum. Thus, in the limit $T\rightarrow 0$, all electronic states at the chemical potential (μ) become Anderson localized (due to disorder) within the bulk of the sample, except for special cases when μ intersects an equipotential which extends across the whole sample. Meanwhile, there exists a fixed number of extended states at the edges of the sample which are robust against scattering by disorder. These ideal one-dimensional conducting states fix the magnitude of the Hall conductance and, therefore, the value of the Hall voltage measured across the sample; hence the term ''quantum Hall conductor.''

Hall resistance quantization has also been observed in bulk systems such as the organic Bechgaard salts.[4] Although strictly (quasi-) three dimensional, the electronic structures of these materials are highly anisotropic, or quasi-one-dimensional (Q1D). Nevertheless, the basic ingredients which give rise to a QHE are essentially the same as those which give rise to the conventional 2D QHE, though the mechanism is entirely different. In the Bechgaard salts, it is the remarkable properties of a field-induced spin-density wave which stabilize the QHE.[5–7] The quantized Hall resistance is brought about by Landau quantization of tiny residual pieces of Fermi surface left over from the imperfectly nested Q1D Fermi surface. These residual Fermi surfaces must be quasi-two-dimensional (Q2D) in order for the magnetic field to produce the clear mobility gaps in their electronic excitation spectrum. Meanwhile, the field-induced spin-density-wave condensate plays the same role as the Anderson-localized states in the conventional 2D QHE, by pinning the chemical potential in these mobility gaps over extended intervals in magnetic field.

The extent to which the similarities between 2D and bulk quantum Hall systems extend is still unclear. Recent theoretical studies have suggested that edge effects may be equally important in the bulk QHE.[8,9] In fact, a novel form of conductor is expected to exist at the edges of layered 2D systems which exhibit a QHE; interlayer tunneling creates a situation where the edge states due to each individual 2D layer become weakly coupled, giving rise to a chiral sheath of current carrying states enveloping the sample. The properties of this 2D system are expected to be highly anisotropic: parallel to the applied field, the transport is predicted to be diffusive and independent of scattering length, leading to a temperature independent ρ_{zz} as $T\rightarrow 0$; meanwhile, the transport perpendicular to the field is expected to be ballistic with vanishing ρ_{xx} as $T\rightarrow 0$. Experimental evidence for these edge effects are beginning to appear in the literature.[10–12]

There is, however, one major difference between bulk and purely 2D quantum Hall systems. Due to a finite bandwidth in the direction parallel to the magnetic field, there exist extended ranges in energy (or magnetic field) over which the

chemical potential may reside among mobile electronic states for bulk QHE systems. Thus the phase diagram for a bulk QHE system might look something like the schematic in Fig. 1, where quantized Hall phases are separated by metallic Landau bands.

In this paper, we present convincing evidence for a bulk QHE in the inorganic charge-density-wave (CDW) conductor η-Mo_4O_{11}. Magnetotransport measurements reveal all of the usual features associated with the QHE, i.e., very deep minima (~ 0) in the transverse diagonal resistance (R_{xx}) which are coincident with plateaux in the Hall resistance (R_{xy}). This represents the first observation of the QHE in a truly bulk inorganic conductor. In the light of these findings, it is natural to compare and contrast η-Mo_4O_{11} with other systems exhibiting a QHE. In doing so, we make a legitimate case for η-Mo_4O_{11} as a viable system for gaining further insight into the properties of bulk quantum Hall systems.

II. η-Mo_4O_{11}

Molybdenum bronzes and oxides have become the subject of considerable interest due to their low electronic dimensionality and consequent Peierls instabilities, which lead to charge-density-wave ground states.[13,14] Of these, monoclinic η-Mo_4O_{11} consists of layers of MoO_6 octahedra, parallel to (100), separated by MoO_4 tetrahedra, giving rise to a Q2D electronic structure.[13] The room-temperature Fermi surface of η-Mo_4O_{11} has been calculated using a tight-binding method;[15,16] both electron and hole pockets elongated along the a^* axis are predicted, in agreement with recent experiments.[17] Within the *bc* plane, the electronic properties show considerable anisotropy, reflecting a ''hidden'' Q1D character which is related to the presence of conducting chains along the *b* and $b \pm c$ crystallographic directions.[16,18] A consequence of this ''hidden'' one dimensionality is that η-Mo_4O_{11} undergoes two successive CDW transitions: the first at 109 K, followed by a second at $\sim$30 K.[13] Each transition nests large sections of the room-temperature Fermi surface, leaving very small, highly two-dimensional, hole and electron pockets at low temperatures.[19]

In a previous study, considerable insight into the ground-state electronic structure of η-Mo_4O_{11} was achieved.[19] Indeed, the possibility of observing a QHE was discussed. In particular, the striking similarity between η-Mo_4O_{11} and the semimetallic InAs/GaSb superlattice system with closely matched electron and hole densities was noted.[20] Both systems may be thought of as arrays of weakly coupled 2D electron systems. What is more, they have similar band-structure parameters and mobilities. As a result, both materials exhibit spectacular magnetic quantum oscillations, and both undergo a field-induced transition from a semimetallic to a semiconducting state when the quantum limit is reached and the hole and electron bands uncross.[19] It is these properties of η-Mo_4O_{11} which have motivated the present study, namely, the possibility of observing a QHE in a Q2D layered system in reasonable laboratory fields, i.e., $<$20 T.

III. EXPERIMENTAL DETAILS

Single crystals of η-Mo_4O_{11} were grown by a vapor-transport technique;[19,21] they form as small platelets

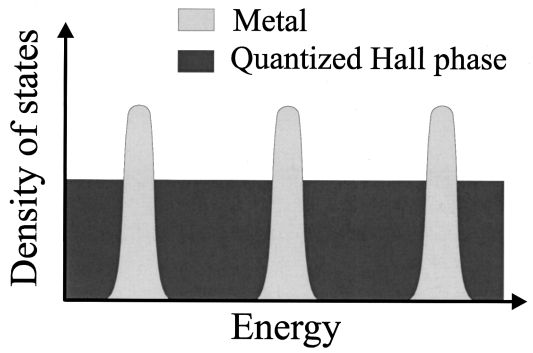

FIG. 1. Schematic phase diagram for an anisotropic quasi-three-dimensional conductor in a quantizing magnetic field.

($\sim 1 \times 0.5 \times < 0.1$ mm^3) with the platelet plane defined by the *bc* plane. Several different samples from two separate batches were studied, thereby providing a high level of confidence in our results. Resistance measurements were made using standard four terminal ac lock-in techniques through gold wires attached to the sample with conductive paint. Contact resistances were typically of the order of a few Ω, and excitation currents in the range 50 μA (dilution fridge) to 200 μA (^{3}He fridge) were used.

For measurements of the in-plane (*bc* plane) resistance tensor, four contacts were placed on the thin edges of the sample, while the longitudinal, or a^*-axis resistance (R_{zz}), was measured by means of pairs of contacts on opposite faces of the platelike samples. A current $I_{m,n}$ was then passed through the sample via contacts *m* and *n*, and a potential difference $V_{p,q}$ was measured across the sample between a different set of contacts *p* and *q*.

For in-plane measurements, the ratio $V_{p,q}/I_{m,n}$ yields a

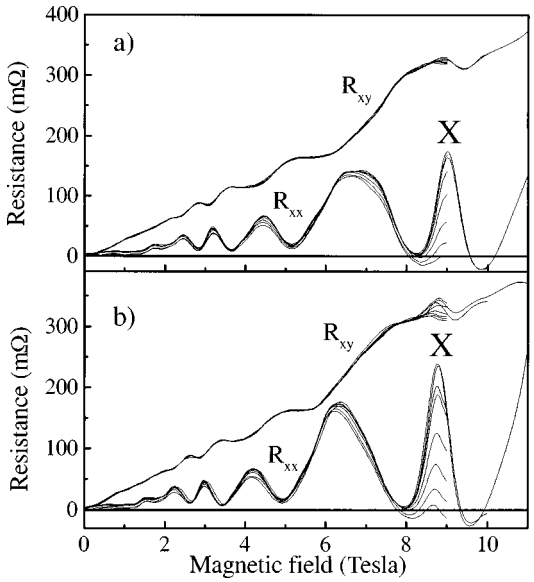

FIG. 2. Temperature dependence of R_{xx} and R_{xy} (sample No. 1) for (a) up-sweeps, and (b) down-sweeps of the magnetic field. The strongly temperature-dependent features are artifacts (see text). The data were taken at more-or-less evenly spaced intervals in temperature from 900 to 70 mK; the lowest temperature data have the largest R_{xx} maxima. Note the considerable hysteresis between up- and down-sweeps of the magnetic field.

resistance which is an admixture of both diagonal and off-diagonal components of the resistance tensor. These contributions may be separated according to the reciprocity principle.[22] Reversing the direction of the applied magnetic field changes the sign of the Hall voltage, but not the dissipative voltage. Thus symmetric and asymmetric averages of the resistances measured with the magnetic field applied parallel and antiparallel to the a^* axis yield the diagonal and transverse Hall (R_{xy}) components of the resistance tensor, respectively. This procedure is not necessary when measuring R_{zz}, since it is several orders of magnitude greater than any other component of the resistance tensor when measured in this way.

Experiments were carried out at the National High Magnetic Field Laboratory in Florida, and at the National Research Institute for Metals in Tsukuba, Japan. The majority of the measurements were conducted in superconducting solenoids and dilution refrigerators, though resistive magnets and a ^{3}He refrigerator were also employed for some experiments.

IV. EXPERIMENTAL RESULTS

Figure 2 shows a series of measurements of R_{xx} and R_{xy} for sample No. 1, at temperatures below 1 K. Extended regions over which the Hall-effect data are reasonably flat (i.e., plateaulike) can clearly be seen at fields of ~3, 4, 5.5 and 8–10 T in Fig. 2(a) [slightly lower in Fig. 2(b)]. For the most part, the temperature dependence of R_{xy} is extremely weak, except around ~9 T. Similarly, the temperature dependence of R_{xx} is weak except in the vicinity of 9 T. The strongly temperature-dependent feature in R_{xx} (at 9 T), and the irregular form of the highest field R_{xy} plateau, are experimental artifacts which are discussed further below.

It is apparent from Fig. 2 that there is considerable hysteresis between up- and down-sweeps of the magnetic field. This has been well documented for this material, and can been attributed to pinning of a field-dependent CDW.[19] Unfortunately, the hysteresis affects the averaging technique used to obtain R_{xx} and R_{xy}, which may explain the rounding off of the Hall plateaux and the deviations from perfect zeros in R_{xx}. Nevertheless, the field dependence of the CDW turns out to be essential to the existence of a QHE in η-Mo_4O_{11}.

Figure 3(a) shows the temperature dependence of R_{zz} obtained over a similar temperature range as the data in Fig. 2, though for a different sample (No. 2). These data are consistent with previous measurements,[19] and will be used to make comparisons between R_{zz}, R_{xx}, and R_{xy}. Figure 3(b) shows a superposition of the lowest temperature data from Figs 2 and 3(a). When plotted in this manner, it immediately becomes apparent that the strongly temperature-dependent feature at 9 T in Fig. 2 (labeled *X*) is correlated with the R_{zz} peak at 9 T in Fig. 3(a). Not surprisingly, the symmetric averaging procedure used to obtain R_{xx} is unable to separate the longitudinal (R_{zz}) and transverse (R_{xx}) diagonal components of the resistance tensor. Nevertheless, the independent measurement of R_{zz} provides an alternative means of distinguishing between R_{zz} and R_{xx}. Removal of R_{zz} from the data in Fig. 2 reveals a broad minimum (~0) around 9 T which is coincident with a region where the slope of R_{xy} is extremely shallow, i.e., plateaulike—this is shown in Fig. 4.[23]

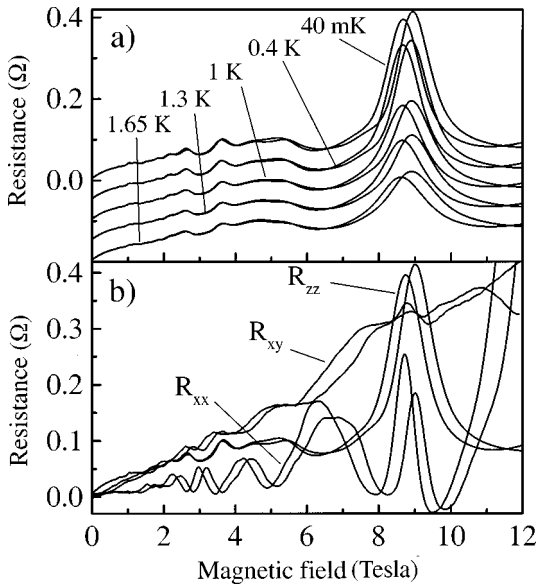

FIG. 3. (a) Temperature dependence of R_{zz} for sample No. 2 (offset for clarity), and (b) a comparison between the lowest temperature R_{xx}, R_{xy} (Fig. 2) and R_{zz} data.

Above 11 T, R_{xx} increases sharply (Fig. 4), while the slope of R_{xy} changes sign. This behavior is consistent with our earlier work (Ref. 19; see also Fig. 5) and is associated with the transition to a semiconducting state. Incidentally, these earlier measurements were performed on thicker samples; the Hall resistance, at 9 T, in the present sample (No. 2) is more than an order of magnitude greater than in previous studies, which probably explains why well-defined R_{xy} plateaux and R_{xx} minima have not been observed until now. The reason for the poorly quantized Hall resistance at 9 T may be attributed to increased hysteresis above about 6 T, and the fact that R_{xx} increases sharply above 9 T. These factors, together with the strongly temperature-dependent admixture of R_{zz} in the raw signal, greatly increase the uncertainty in the asymmetric averaging method used to obtain R_{xy} above about 8 T. These factors are also responsible for

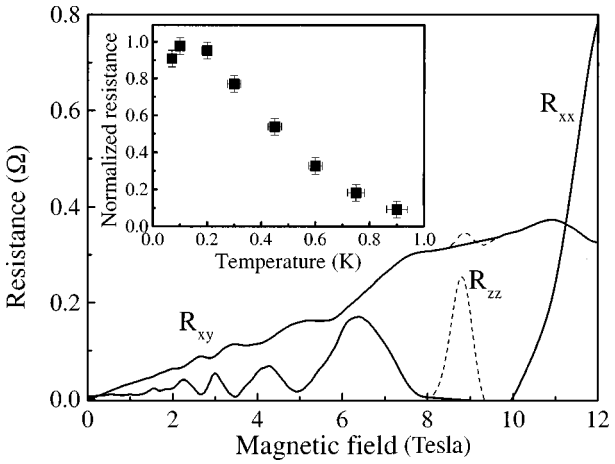

FIG. 4. Corrected R_{xy} and R_{xx} data for sample No. 1 ($T = 100$ mK). The inset shows the temperature dependence of the resistance peak attributed to R_{zz} at 9 T (dashed line in main part of figure); these data have been normalized to the value of the peak resistance in the main part of the figure.

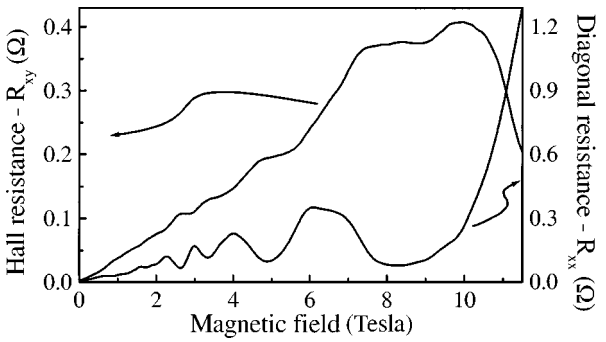

FIG. 5. R_{xy} and R_{xx} data for a third sample (No. 3). The data were taken from down-sweeps and the temperature was 100 mK.

the negative values of R_{xx} seen in Fig. 2.

The inset to Fig. 4 shows the temperature dependence of the 9 T R_{zz} resistance maximum (from sample No. 2). Previous studies have indicated that R_{zz} is activated in the vicinity of 9 T, and at temperatures above about 500 mK.[19] The present data show that R_{zz} tends to saturate and even decrease somewhat below about 300 mK.

Figure 5 shows raw R_{xy} data for a third sample (No. 3) which is in good agreement with the data in Figs. 2 and 4. Sample No. 3 was cleaved from the same polycrystal as sample No. 1. It is interesting to note that the absolute Hall plateau resistances at ~9 T are similar for sample Nos. 1 and 3, i.e., ~0.32 and 0.38 Ω, respectively (note that these values are averages from many measurements, with errors of ± 5 mΩ). It is expected that these resistances scale inversely with the thickness' of the two samples, which, indeed, turns out to be the case to within the experimental error. The thickness' of sample Nos. 1 and 3 are 50 and 40 μm (± 5 μm), respectively; thus the product thickness times the Hall resistance is 16 ± 3 and 15.2 ± 3 for sample Nos. 1 and 3, respectively.

In order to determine the filling factor corresponding to each Hall plateau, we plot the inverse of R_{xy} for a fourth sample (No. 4) against the inverse magnetic field (Fig. 6). Again, well-defined plateaux are observed and, as with sample No. 1, there is no discernible temperature dependence in R_{xy} at these low temperatures. The data have been normalized with respect to the 9 T Hall plateau in order to demonstrate that quantization occurs in units of the 9 T Hall

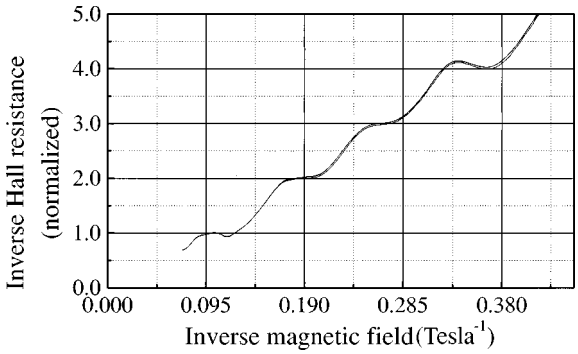

FIG. 6. Inverse Hall effect $(R_{xy})^{-1}$ data for sample No. 4 at 125, 220, and 400 mK (overlaid). $(R_{xy})^{-1}$ has been normalized to its value at 9 T in order to demonstrate the excellent quantization. Note that the Hall plateaus do not occur at integer multiples of the value of the inverse magnetic field at the last resistance plateau.

conductance;[24] i.e., when normalized and plotted in this way, plateaux occur at integer multiples of the inverse Hall resistance at 9 T. Thus we conclude that the Hall plateau at 9 T is the last, representing the situation where only one Landau level (or set of unresolved Landau levels) is occupied. These findings are in fair agreement with our earlier measurements.[19] However, closer examination of Fig. 6 reveals that the Hall plateaux do not occur at regular intervals in inverse magnetic field. This latter observation is rather anomalous and may be attributed to the field-dependent CDW which results in a field-dependent carrier density (see below).

Finally, we compare the measured Hall resistances with the fundamental Hall resistance quanta h/e^2—the Klitzing. Taking as an example sample No. 3, which has a thickness of 40 ± 5 μm, and assuming a value for the unit cell dimension normal to the conducting layers of 24.5 Å, we deduce that a maximum of ~16 330 layers contribute to the measured Hall voltage. Thus, if all of the layers in the sample contribute to the Hall effect, the quantized Hall resistance at the last Hall plateau should be 1.58 ± 0.2 Ω, which, to within the experimental error, is four times the measured value. This difference cannot be explained by a redundancy of some of the 2D layers within the sample, since this would give rise to a larger than expected Hall resistance.

V. DISCUSSION

First, we discuss a possible mechanism for the bulk QHE in η-Mo_4O_{11}. Our previous investigations have determined that the ground-state Fermi surface is highly 2D—one prerequisite for the QHE.[19] Therefore, all that is required is some means of pinning the chemical potential between Landau bands over extended intervals in magnetic field. This can be achieved by any reservoir of immobile states which is capable of exchanging carriers with the mobile 2D states. By immobile, we mean states which do not contribute to dc transport. Clearly, a likely candidate in η-Mo_4O_{11} is the CDW condensate. The observed hysteresis (Fig. 2) indicates that the CDW wave vector shifts upon application of a magnetic field.[19] As it does so, the 2D carrier density also changes, since the CDW wave vector determines the nesting properties of the unnested Fermi surface. In fact, this effect is quite dramatic as shown by the strongly field-dependent periodicity of the Hall plateaux in Fig. 6. This is a clear demonstration of the fact that carrier density has absolutely nothing to do with the QHE apart from fixing the positions of the Hall plateaux in field, i.e., Hall resistance quantization is robust in this situation.

This mechanism, involving the exchange of carriers between mobile 2D states and the localized charge-density-wave condensate, is analogous to the situation which gives rise to a QHE in the Bechgaard salts.[5–7] This would seem to suggest that the QHE is a natural property of imperfectly nested density-wave conductors. Indeed, indirect evidence exists for a QHE in some of the Q2D organic charge-transfer salts with spin-density waves.[10,11]

We next turn to the maximum observed Hall resistance, which corresponds to one quarter of a Klitzing per 2D layer. Accounting for a factor of 2 is trivial if the spin degrees of freedom within each Landau band are not resolved.[2] To ex-

plain the factor of 4 requires the introduction of an additional degeneracy of 2 among the electronic states of the system. It is possible that this extra degeneracy arises because there are two 2D conducting layers for each MoO_6 layer in crystal structure. Clearly, further low-temperature studies will be required to resolve this issue.

For a QHE to be observed at all in a bulk material, the Q2D Landau bands shown in Fig. 1 must be clearly resolved from each other. In η-Mo_4O_{11}, the high degree of two dimensionality, low carrier effective masses ($\sim 0.1 m_e$), and a high mobility create these necessary conditions.[19] The low effective mass leads to a cyclotron splitting between the centers of adjacent Landau bands of $\sim$1 meV per T. From these numbers, and from the widths of the transitions between Hall plateaux (Fig. 2), we estimate the a^*-axis bandwidth to be of order 1–2 meV [$\simeq (10-20) k_B$]. Although rather low, this value explains the nonresolution of spin-splitting of the Landau bands, and the weak temperature dependence of the data. Estimates of the g factor in η-Mo_4O_{11} indicate that it cannot be substantially greater than the free-electron value $g=2$.[19,25] Thus the spin splitting is not expected to exceed $\sim$1 meV at 10 T, a value which is less than the width of the Landau bands. In hindsight, it is clear that little temperature dependence in R_{xx} and R_{xy} should be expected until the temperature scale becomes comparable to the Landau bandwidth, i.e. on the order of a few K. Thus the QHE in η-Mo_4O_{11} should persist to relatively high temperatures.

Turning to R_{zz} in Fig. 3(a), the strong temperature dependence at 9 T is indicative of the fact that the bulk of the sample is completely insulating. There is excellent agreement between R_{xx}, R_{xy}, and R_{zz} at this point [Fig. 3(b)], where peaks in R_{zz} coincide perfectly with the Hall plateaux. The reason for the minima in R_{xx} at these instances is not related to what is happening in the bulk of the sample, which is insulating, but to the sample edges where dissipationless edge channels supposedly reside. Thus, in a quantized Hall phase, the in-plane and interplane transport properties appear to have nothing to do with each other—one probes the bulk and the other the edges of the sample (we re-examine this situation further below). Away from the Hall plateaux R_{xx} increases due to dissipation in the bulk of the sample, while R_{zz} decreases as a result of the chemical potential, coinciding with states which are mobile along the a^* axis.

The above behavior can be summed up with reference to Fig. 1. When the chemical potential coincides with a Landau band, the system behaves like an anisotropic metal, i.e., the diagonal components of the resistance tensor show metallic character, and R_{xy} is not quantized. To demonstrate this, we plot the temperature dependence of R_{zz} at 0, 6.5 and 13 T, in Fig. 7(a); these fields correspond to situations where the chemical potential coincides with a Landau band.[26] As expected, R_{zz} is metalliclike at the lowest temperatures, i.e., R_{zz} decreases with decreasing temperature. Conversely, when the chemical potential resides between Landau bands (in a quantized Hall phase), the in-plane transport properties are dominated by edge channels, whereas the interplane transport properties show semiconducting behavior. This is illustrated in Fig. 7(b), where the temperature dependence of R_{zz} is shown at fields where R_{xy} plateaux are observed (see, e.g., Fig. 2). Once again, the expected behavior is seen at the lowest temperatures, i.e., in these cases, the resistance increases with decreasing temperature. One final point to note: the slope of R_{zz} versus temperature is seen to oscillate in some of the traces. This behavior suggests that the CDW wave vector and, therefore, the carrier density is temperature dependent as well as field dependent. Thus the phase diagram for η-Mo_4O_{11} is quite complex.

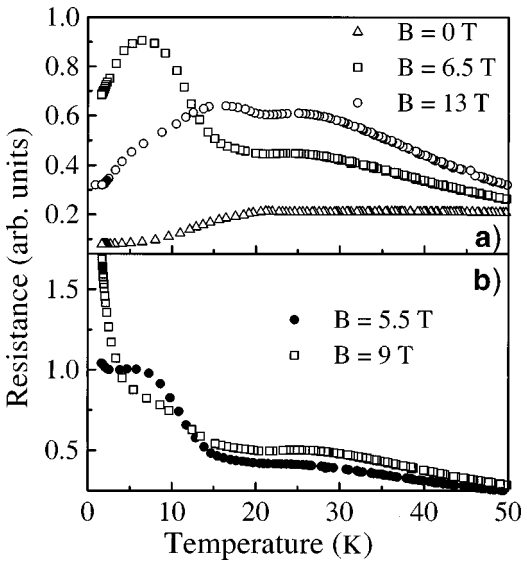

FIG. 7. (a) Temperature dependence of R_{zz} when the chemical potential coincides with a Landau band. (b) Temperature dependence of R_{zz} in a quantum Hall phase.

The reason for the admixture of R_{zz} and R_{xx}, as seen for the in-plane measurements in Fig. 2, is most probably due to imperfect contacts to the sample. Ideally, these contacts should connect to every layer. However, in practice, currents may flow between layers in order to reach other layers which are not well connected to the contacts (Note that the measured Hall plateau resistances would seem to indicate that all of the layers are involved.) At first sight, this may seem undesirable. However, since R_{xx} is, in principle, zero whenever R_{zz} is maximum, this presents an extremely effective way of measuring R_{zz} close to the edges of the sample when the bulk of the sample is insulating. This ties in nicely with the predictions concerning the transport of current along the a^* axis via surface states.[8,9]

As discussed in Sec. I, Balents and Fisher predicted that, in layered samples which exhibit a bulk QHE, a 2D chiral metallic ribbon should exist at the edge of the sample.[9] At low temperatures, this surface layer should dominate the z-axis transport (i.e., parallel to the field) once the bulk of the sample becomes completely insulating. We propose that this may be one possible explanation for the saturation of R_{zz} at low temperatures, as seen in Fig. 4. Clearly, further investigations are necessary to determine if this is the case. Nevertheless, we believe that η-Mo_4O_{11} represents an ideal system to explore these ideas further.

VI. SUMMARY

We present convincing evidence for a bulk QHE in η-Mo_4O_{11}. Magnetotransport measurements reveal all of the usual features associated with the QHE, i.e., very deep minima ($\sim$ zeros) in the transverse diagonal resistance (R_{xx})

which are coincident with plateaus in the Hall resistance (R_{xy}). This represents the first observation of the QHE in a truly bulk inorganic conductor. We show data for several different samples and contact geometries, and find good agreement between the behavior of each component of the resistance tensor.

We propose a model along similar lines to the standard model used to explain the QHE in the Bechgaard salts.[5–7] This involves tiny quasi-two-dimensional electron and hole pockets, left over from an imperfectly nested charge-density wave, and the exchange of carriers between these mobile states and the localized charge-density-wave condensate. These factors result in well-separated bands of mobile states superimposed on a background continuum of localized states, when the sample is subjected to a perpendicular magnetic field.

We also discuss the implications of our findings in the light of recent predictions concerning chiral metallic surface states in bulk quantum Hall systems. In doing so, we make a legitimate case for η-Mo_4O_{11} as a viable system for gaining further insight to the properties of bulk quantum Hall systems.

ACKNOWLEDGMENTS

This work was supported by NSF Grant No. DMR-95-10427 and in part by NSF cooperative agreement No. 98-71922. The National High Magnetic Field Laboratory is supported by NSF cooperative agreement No. DMR-95-27035.

[1] K. von Klitzing, G. Dorda, and M. Pepper, Phys. Rev. Lett. **45**, 494 (1980).

[2] *The Quantum Hall Effect*, edited by R. E. Prange and S. M. Girvin (Springer-Verlag, Berlin, 1987).

[3] T. Chakraborty and P. Pietilainen, *The Quantum Hall Effects—Fractional and Integer*, Springer Series in Solid-State Sciences, Vol. 85 (Springer, Berlin, 1995).

[4] S. T. Hannahs, J. S. Brooks, W. Kang, L. Y. Chiang, and P. M. Chaikin, Phys. Rev. Lett. **63**, 1988 (1989).

[5] L. P. Gor'kov and A. G. Lebed, J. Phys. (Paris) Lett. **45**, L433 (1984).

[6] P. M. Chaikin, W. Kang, S. Hannahs, and R. C. Yu, Physica B **177**, 353 (1992).

[7] G. Montambaux, Physica B **177**, 339 (1992).

[8] J. T. Chalker and A. Dohmen, Phys. Rev. Lett. **75**, 4496 (1995).

[9] L. Balents and M. P. A. Fisher, Phys. Rev. Lett. **76**, 2782 (1996).

[10] N. Harrison, A. House, M. V. Kartsovnik, A. V. Polisski, J. Singleton, F. Herlach, W. Hayes, and N. D. Kushch, Phys. Rev. Lett. **77**, 1576 (1996).

[11] S. Hill, P. S. Sandhu, J. S. Qualls, J. S. Brooks, M. Tokumoto, N. Kinoshita, T. Kinoshita, and Y. Tanaka, Phys. Rev. B **55**, R4891 (1997).

[12] D. P. Druist, P. J. Turley, K. D. Maranowski, E. G. Gwinn, and A. C. Gossard, Phys. Rev. Lett. **80**, 365 (1998).

[13] *Low Dimensional Electronic Properties of Molybdenum Bronzes and Oxides*, edited by C. Schlenker (Kluwer, Dordrecht, 1989), and references therein.

[14] R. E. Thorne, Phys. Today **49** (5), 42 (1996).

[15] E. Canadell, M-H. Whangbo, C. Schlenker, and C. Escribe-Filippini, J. Inorg. Chem. **28**, 213 (1989).

[16] E. Canadell and M-H. Whangbo, Chem. Rev. **91**, 965 (1991).

[17] M. Sasaki, G. X. Tai, S. Tamura, and M. Inoue, Phys. Rev. B **47**, 6216 (1993).

[18] M. H. Whangbo, E. Canadell, P. Foury, and J.-P. Pouget, Science **252**, 96 (1991).

[19] S. Hill, S. Valfells, S. Uji, J. S. Brooks, G. J. Athas, P. S. Sandhu, J. Sarrao, Z. Fisk, J. Goettee, H. Aoki, and T. Terashima, Phys. Rev. B **55**, 2018 (1997).

[20] M. S. Daly, K. S. H. Dalton, M. Lakrimi, N. J. Mason, R. J. Nicholas, M. van der Burgt, P. J. Walker, D. K. Maude, and J. C. Portal, Phys. Rev. B **53**, R10 524 (1996).

[21] M. Inoue, S. Ohara, S. Horisaka, M. Koyano, and H. Negishi, Phys. Status Solidi B **148**, 659 (1988).

[22] H. H. Sample, W. J. Bruno, B. B. Sample, and E. K. Sichel, J. Appl. Phys. **61**, 1079 (1987).

[23] To obtain this figure, we simply removed the offending 9-T features from R_{xx} and R_{xy}, and then interpolated between appropriate points either side of this range.

[24] Although $(R_{xy})^{-1}$ does not strictly yield the Hall conductance for all values of the magnetic field, we assume that it does so at the Hall plateaus, where R_{xx} is negligible.

[25] S. Hill *et al.* (unpublished).

[26] 13 T corresponds to the point at which the chemical potential coincides with the lowest Landau band. This is in fair agreement with our earlier estimates for the quantum limit in Ref. 19.